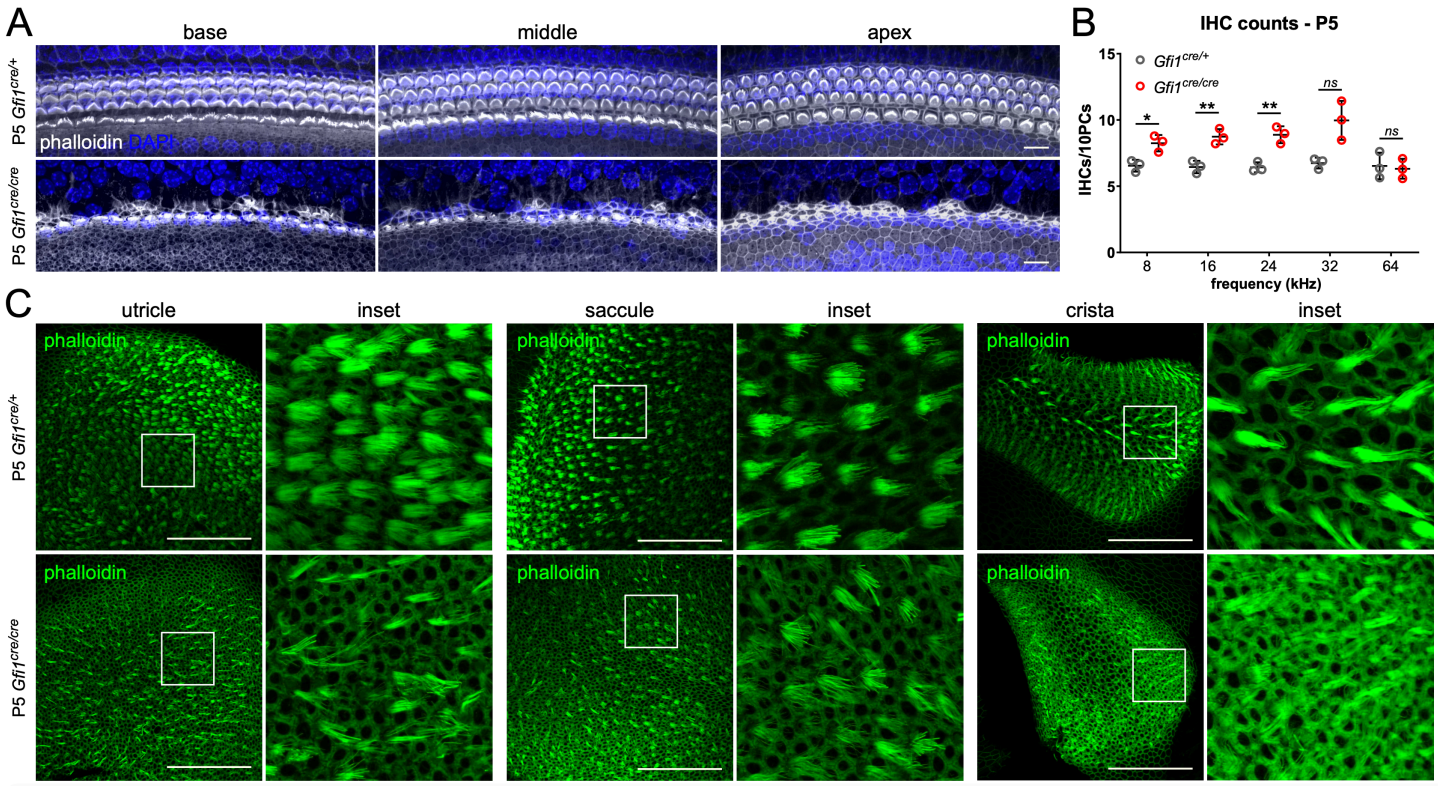

Fig.S1. Progressive OHC degeneration and thinner vestibular hair bundles in the P5 GFI1 mutant inner ear. (A) Phalloidin staining of HC bundles at P5 showed progressive OHC degeneration compared to P0 (n=3). Scale=20μm. **(B)** Quantification of IHCs at P5 revealed an increase in IHCs in both the middle and apical turns of the *Gfi1*$^{cre/cre}$ cochlea (n=3). **(C)** Phalloidin staining demonstrated thinner *Gfi1*$^{cre/cre}$ vestibular HC bundles also at P5 (n=3). Scale=50μm. *=*p*-value<0.05, **=*p*-value<0.01, *ns*=not significant. Statistical significance assessed by Welch's t-test.

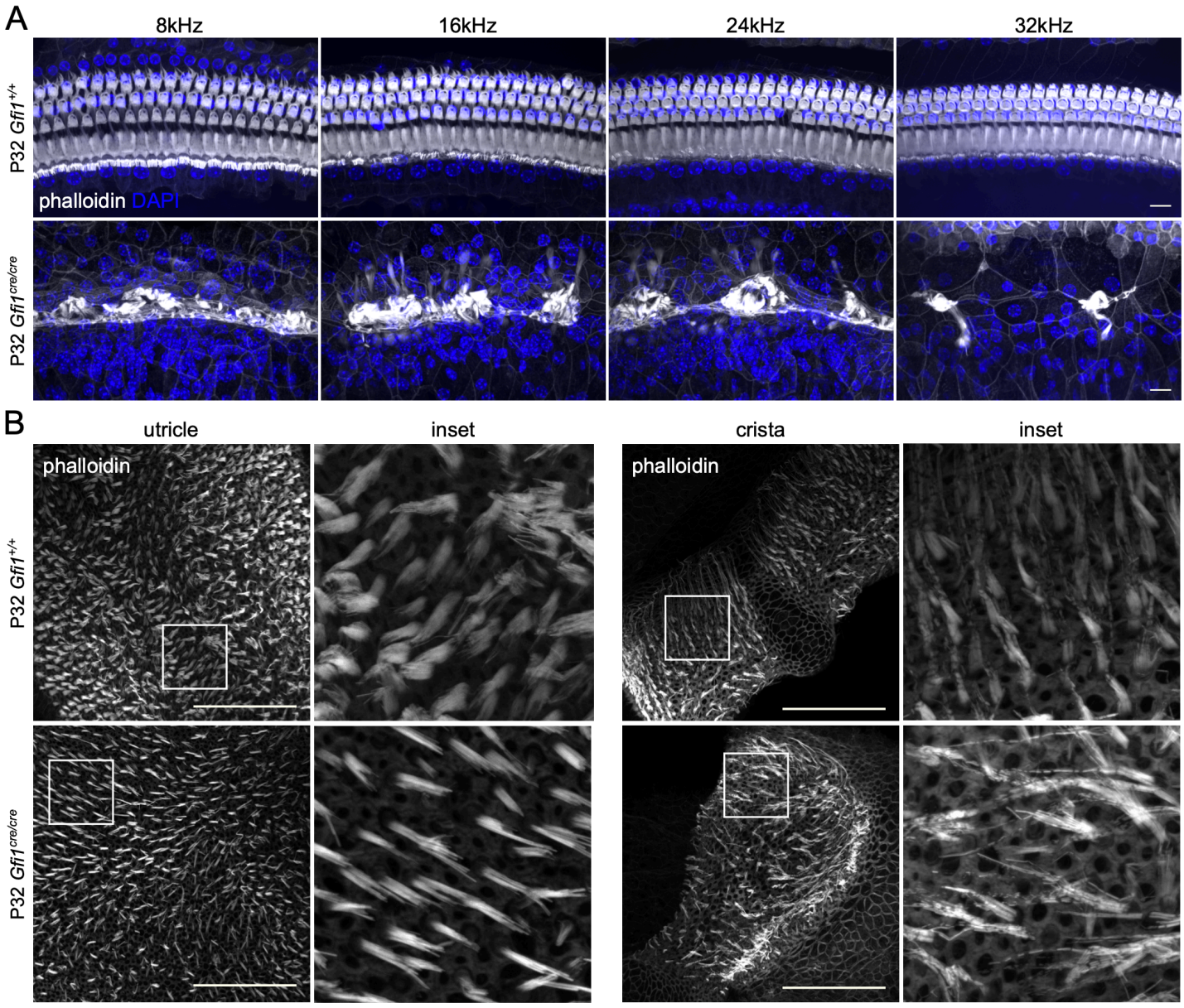

Fig.S2. OHC and IHC degeneration and thinner vestibular hair bundles in the 1 month old GFI1 mutant ears. (A) Phalloidin staining of HC bundles at 1 month showed OHC and IHC degeneration in the *Gfi1* mutants compared to wild type controls (n=3). Scale=20μm. **(B)** Phalloidin staining demonstrated thinner *Gfi1*$^{cre/cre}$ vestibular HC bundles also at 1 month (n=3). Scale=50μm.

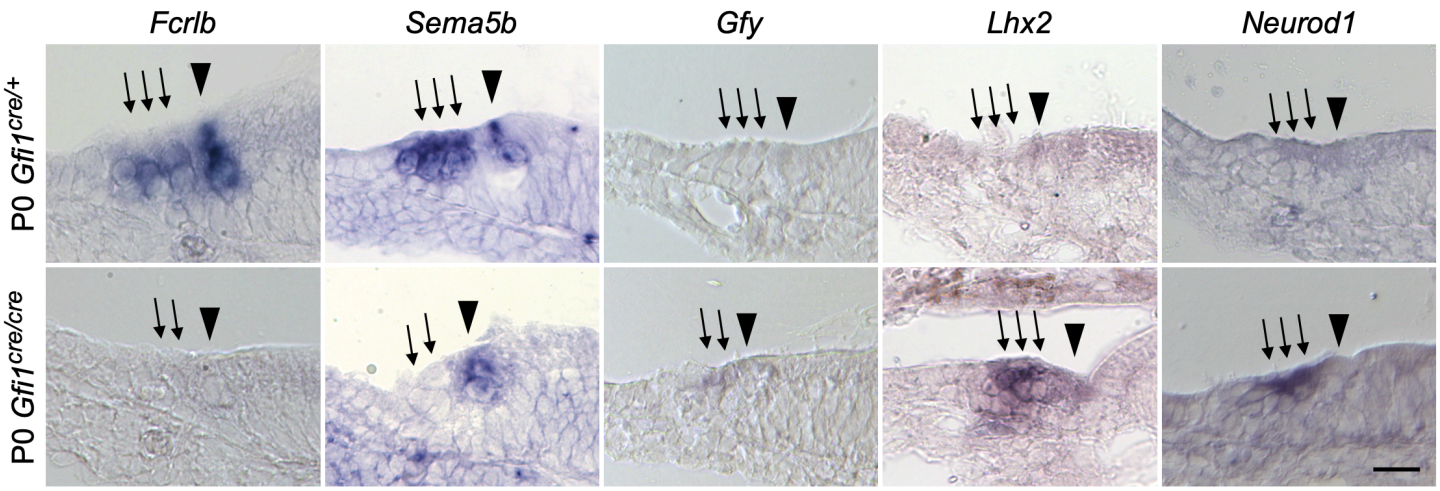

Fig.S3. *In situ* hybridization of HC and neuronal-associated genes in the GFI1 mutant HCs. HC-specific downregulation of *Fcrlb* and *Sema5b*, and upregulation of the neuronal-associated genes *Gfy, Lhx2, Neurod1* in *Gfi1*$^{cre/cre}$ cochlear HCs. Arrowheads denote IHCs, arrows denote OHCs. Scale=20μm.

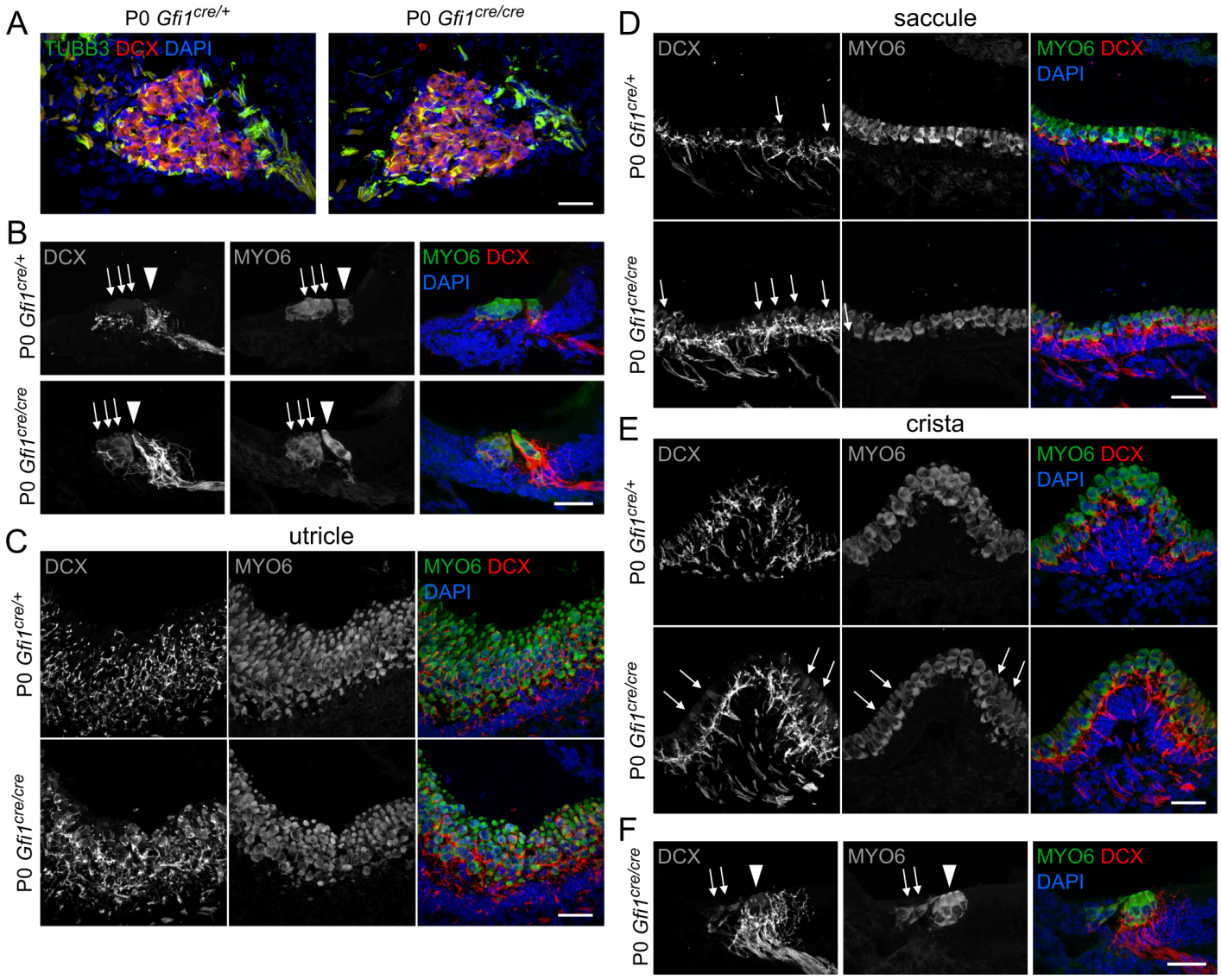

Fig.S4. Upregulation of the neuronal marker DCX (doublecortin) in the GFI1 mutant HCs. (A) DCX is expressed in neurons in both the *Gfi1*$^{cre/+}$ and *Gfi1*$^{cre/cre}$ cochlea. **(B)** DCX is expressed in the *Gfi1*$^{cre/cre}$ OHCs at P0, and overlaps with MYO6 expression (n=3). Arrowheads denote IHCs, arrows denote OHCs. **(C-E)** DCX is expressed in the *Gfi1*$^{cre/cre}$ vestibular HCs at P0. Occasionally, DCX staining was seen in vestibular HCs of the *Gfi1*$^{cre/+}$ animals (see D, saccule), but not to the extent of *Gfi1*$^{cre/cre}$. (n=3, arrows denote DCX expression in HCs). **(F)** Occasionally, DCX staining was also observed in *Gfi1*$^{cre/cre}$ IHCs. Scale=20μm.

Table S1. RNA-seq dataset measuring changes in gene expression between *Gfi1*$^{cre/cre}$ (HOM) and *Gfi1*$^{cre/+}$ (HET) cochlear hair cells in biological triplicate using RiboTag immunoprecipitation. In addition to a cutoff of Log2 fold change (logR.Hom.vs.Het) > 1 or < -1 and false discovery rate (FDR) < 0.001, we required a full separation (Separation = Yes) of normalized expression values between replicates to call a gene as differentially expressed (DE, see methods for more detail).

Click here to Download Table S1

Table S2. RNA-seq dataset measuring changes in gene expression between *Gfi1*$^{cre/cre}$ (HOM) and *Gfi1*$^{cre/+}$ (HET) vestibular hair cells in biological triplicate using RiboTag immunoprecipitation. In addition to a cutoff of Log2 fold change (logR.Hom.vs.Het) > 1 or < -1 and false discovery rate (FDR) < 0.001, we required a full separation (Separation = Yes) of normalized expression values between replicates to call a gene as differentially expressed (DE, see methods for more detail).

Click here to Download Table S2

#Sample ID	Total Reads	Total Mapped Reads	Percent Mapped Reads	Percent Properly Paired	Uniquely Mapped Reads	Percent Exonic	Percent Intronic	Percent Intergenic
HetIPV1	198797686	140034819	70.44	87.34	130007929	88.05	7.11	4.84
HetIPV1.down		75665746			72822796	86.81	7.35	5.84
HetIPV2	78107408	58755404	75.22	87.33	55775036	82.53	12.29	5.18
HetIPV3	93486052	71921316	76.93	88.05	68268206	82.83	12.49	4.68
HomIPV1	235153252	166579597	70.84	86.18	157536060	89.24	5.89	4.87
HomIPV1.down		60081940			58636144	87.81	6.25	5.93
HomIPV2	74915388	56582744	75.53	87.7	52905966	85.74	9.33	4.93
HomIPV3	80757870	58920296	72.96	86.5	56051712	83.13	11.03	5.83
HetIPC1	63936396	44112209	68.99	79.88	43254231	33.73	59.96	6.31
HetIPC2	67494692	45216432	66.99	79.41	44399585	31.3	62.62	6.08
HetIPC3	72095906	49467639	68.61	79.47	48571130	35.56	58.63	5.81
HomIPC1	70224610	49291915	70.19	80.62	48463724	30.59	63.46	5.95
HomIPC2	63536374	43675854	68.74	79.93	42822328	33.54	60.22	6.24
HomIPC3	68056790	46975426	69.02	79.33	46137061	34.32	59.76	5.91

Table S3. Alignment statistics for *Gfi1*$^{cre/cre}$ and *Gfi1*$^{cre/+}$ RiboTag RNA-seq replicates. HetIPC = *Gfi1*$^{cre/+}$ immunoprecipitated RNA from cochlea, HomIPC = *Gfi1*$^{cre/cre}$ immunoprecipitated RNA from cochlea, HetIPV = *Gfi1*$^{cre/+}$ immunoprecipitated RNA from vestibule, HomIPV = *Gfi1*$^{cre/cre}$ immunoprecipitated RNA from vestibule. Upon noticing the high percent intronic reads obtained when using the Ovation® Ultralow Library Preparation Kit (NuGEN) for the cochlear IP sample, we switched to using the NEBNext® Ultra™ Directional RNA Library Prep Kit (New England BioLabs) for the vestibular IP samples. This resulted in a much lower percentage of intronic reads sequenced, consistent with the observations presented in Song et al., 2018. Additionally, two vestibular samples (HetIPV1, HomIPV1) were sequenced to a higher depth and randomly down sampled for our analysis (HetIPV1.down, HomIPV1.down).

TaqMan probes		
Actb Mm12619580_g1; *Tbp* Mm01277042_m1; *Myo6* Mm00500651_m1; *Tubb3* Mm00727586_s1; *Pou3f4* Mm00447171_s1; *Fcrlb* Mm01295310_g1; *Ocm* Mm00712881_m1; *Atoh1* Mm00476035_s1; *St18* Mm01236999_m1; *Gfy* Mm04243347_g1; *Cdh1* Mm01247357; *Sema5b* Mm00443163_m1; *Slc26a5* Mm00446145_m1; *Strc* Mm01328720_m1; *Strip2* Mm00623363; *Gap43* Mm00500404_m1; *Tmc1* Mm00452982_m1; *Myt1* Mm00456190_m1; *Ncam1* Mm01149710_m1; *Lhx2* Mm00839783_m1; *Neurod1* Mm01280117_m1; *Insm1* Mm02581025_s1.		
ISH probe primers		
Gene name	**Forward**	**Reverse**
Neurod1	ACCTTTTAACAACAGGAAGTGGA	GGGGACTGGTAGGAGTAGGG
Gfy	CACTCCCAAGAATCCCTGAA	GGTTGGTTCCAGTGCAGAAT
Lhx2	GAGAGTCCTCCAGGTCTGGTTT	GCGACCGTTGGAGGGGTTT
Fcrlb	GTGGTGCTGCGCTGCGAGAC	CTAGCTGTCCACTCGGCCCTCCA
Sema5b	GGCCTGCCCAGAAGGCTGGTCACTG	CACTGACAAGCTGGACGCAGCCCCG

Table S4. Taqman probes used for qPCR and primers used to generate *in situ* hybridization probes.

Supplementary references

Song, Y., Milon, B., Ott, S., Zhao, X., Sadzewicz, L., Shetty, A., Boger, E. T., Tallon, L. J., Morell, R. J., Mahurkar, A., et al. (2018). A comparative analysis of library prep approaches for sequencing low input translatome samples. *BMC Genomics* **19**, 696.